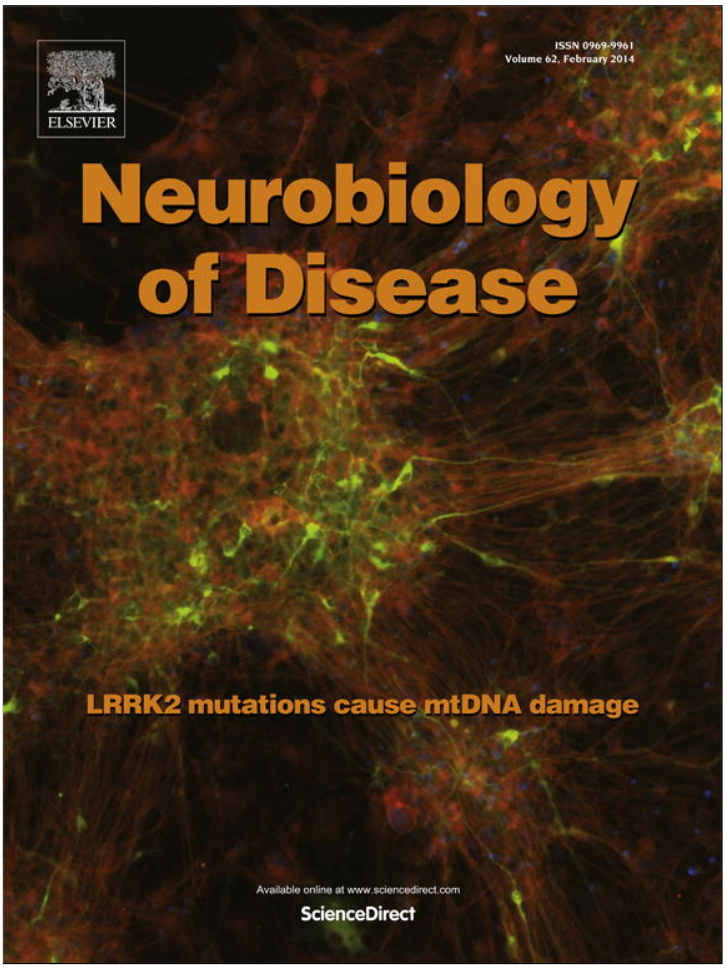

Neurobiology of Disease 62 (2014) 62–72

Contents lists available at ScienceDirect

Neurobiology of Disease

journal homepage: www.elsevier.com/locate/ynbdi

# Efficient derivation of cortical glutamatergic neurons from human pluripotent stem cells: A model system to study neurotoxicity in Alzheimer's disease ☆

Tandis Vazin [a,b,c,h], K. Aurelia Ball [d,h], Hui Lu [c,e,h], Hyungju Park [c,e,h], Yasaman Ataeijannati [f,h], Teresa Head-Gordon [a,b,d,g,h], Mu-ming Poo [c,e,h], David V. Schaffer [a,b,c,h,*]

[a] The Department of Chemical and Biomolecular Engineering, USA
[b] The Department of Bioengineering, USA
[c] Helen Wills Neuroscience Institute, USA
[d] Graduate Group in Biophysics, USA
[e] Division of Neurobiology, Department of Molecular and Cell Biology, USA
[f] Department of Molecular and Cell Biology, USA
[g] Department of Chemistry, USA
[h] University of California, Berkeley, CA 94720, USA

ARTICLE INFO

*Article history:*
Received 19 March 2013
Revised 19 July 2013
Accepted 1 September 2013
Available online 18 September 2013

*Keywords:*
Cortical
Glutamatergic
Neuron
Human
Pluripotent
Stem cell
Amyloid beta
Alzheimer's disease
In vitro model

ABSTRACT

Alzheimer's disease (AD) is among the most prevalent forms of dementia affecting the aging population, and pharmacological therapies to date have not been successful in preventing disease progression. Future therapeutic efforts may benefit from the development of models that enable basic investigation of early disease pathology. In particular, disease-relevant models based on human pluripotent stem cells (hPSCs) may be promising approaches to assess the impact of neurotoxic agents in AD on specific neuronal populations and thereby facilitate the development of novel interventions to avert early disease mechanisms. We implemented an efficient paradigm to convert hPSCs into enriched populations of cortical glutamatergic neurons emerging from dorsal forebrain neural progenitors, aided by modulating Sonic hedgehog (Shh) signaling. Since AD is generally known to be toxic to glutamatergic circuits, we exposed glutamatergic neurons derived from hESCs to an oligomeric prefibrillar forms of Aβ known as "globulomers", which have shown strong correlation with the level of cognitive deficits in AD. Administration of such Aβ oligomers yielded signs of the disease, including cell culture age-dependent binding of Aβ and cell death in the glutamatergic populations. Furthermore, consistent with previous findings in postmortem human AD brain, Aβ-induced toxicity was selective for glutamatergic rather than GABAeric neurons present in our cultures. This *in vitro* model of cortical glutamatergic neurons thus offers a system for future mechanistic investigation and therapeutic development for AD pathology using human cell types specifically affected by this disease.



## Introduction

AD is a neurodegenerative disorder characterized by an abundance of Aβ peptides generated from amyloid precursor abnormal cleavage by membrane-associated secretases (Murphy and LeVine, 2010). The development of AD pathology precedes cognitive symptoms and diagnosis by many years (Lazarczyk et al., 2012), presenting challenges for studying early disease stages to aid in the discovery of preventive drugs.

Over the past decade numerous transgenic animal models of AD have been generated to aid in understanding mechanisms of the disease in humans (Gotz and Ittner, 2008). However, such animals must express multiple pathological proteins at levels higher than endogenous genes to exhibit AD pathology, highlighting the value of developing complementary models to enable investigations in human cells with gene expression patterns closer to endogenous levels. In particular, *in vitro* models derived from hPSCs offer strong platforms for basic research and subsequent therapeutic development for early stages of AD.

Tapping into this potentially exciting new class of disease models requires efficient differentiation of hPSCs into neurons affected by AD. In particular, glutamatergic neurons are severely afflicted in the cerebral cortex, and disruption of their circuits is associated with the hallmark memory deficits of AD (Francis et al., 1993; Greenamyre et al., 1988). In contrast, studies of human postmortem AD brain suggest that

☆ Conflict of interest: The authors declare no competing financial interests.

* Corresponding author at: 278 Stanley Hall, University of California, Berkeley, CA 94720, USA.
*E-mail address:* schaffer@berkeley.edu (D.V. Schaffer).

**Available online on ScienceDirect (www.sciencedirect.com).**

0969-9961/$ – see front matter © 2013 Elsevier Inc. All rights reserved.
http://dx.doi.org/10.1016/j.nbd.2013.09.005

GABAergic neurons are spared from death (Rossor et al., 1982). To date, the sensitivity of human cortical glutamatergic neurons to Aβ has not been studied within *in vitro* models, and such efforts would benefit from renewable sources of glutamatergic neurons derived from hPSCs that could serve as human disease models of AD. We have thus developed an hPSC-based system to examine how Aβ neurotoxicity affects enriched populations of both human cortical glutamatergic and GABAergic neurons.

During development, glutamatergic neurons are generated from the dorsal telencephalon, whereas GABAergic neurons emerge from the ventral telencephalic region (Wilson and Rubenstein, 2000), due in part to Shh-mediated patterning. Here, we show that hESCs and iPSCs differentiated to a dorsal phenotype, with the aid of Shh pathway inhibition and stimulation with FGF-2, primarily give rise to glutamatergic neurons. In contrast, without Shh inhibition, NPCs adapted a ventral phenotype and primarily gave rise a GABAergic fate.

AD is primarily characterized by Aβ plaques; however, amyloid plaque load shows a weak correlation with dementia in AD (Naslund et al., 2000). By comparison, soluble Aβ oligomer levels correlate more closely with AD pathology (Kuo et al., 1996). Thus, a stable, oligomeric Aβ form called "Aβ globulomers" has been prepared and increasingly studied (Barghorn et al., 2005, Gellermann et al., 2008). While human AD brain neuropathology studies show elevated levels of Aβ oligomers surrounding cortical neuronal processes, which may cause synaptic impairment (Viola et al., 2008), the differential neurotoxic effects of these oligomers on different human cortical neuronal populations remain to be elucidated. Such results may enhance our understanding of the contribution of this toxic species to the disease process, aid future elucidation of molecular mechanisms for its actions, and help resolve differences in disease progression between for example familial AD and corresponding animal models (Gotz and Ittner, 2008).

In this study, the derivation of human cortical cultures primarily comprised of glutamatergic neurons enabled investigation of the recently proposed role of Aβ globulomers in AD pathology. Specifically, this intermediate form of Aβ was toxic to human glutamatergic neurons in a cell culture age-dependent manner. Furthermore, the results show that Aβ globulomers exert a selective neurotoxicity for glutamatergic rather than GABAergic neuronal populations.

## Materials and methods

### *Cell culture*

The H1 (WiCell) and HSF6 (UC San Francisco) hESC lines, and the MSC and fibroblast derived iPSC lines (a kind gift from George Q. Daley, Children's Hospital Boston, Boston, MA), were cultured on Matrigel-coated cell culture plates (BD) in mTeSR1 maintenance medium (Stem Cell Technologies). NPCs were isolated from the hippocampus of adult female Fischer 344 rats (Palmer et al., 1999) and cultured in medium containing DMEM/F12 (Invitrogen) supplemented with N2 (Invitrogen) and 20 ng/ml FGF-2 (Peprotech). Neuronal differentiation of adult rat NPCs was achieved by withdrawing FGF-2 and adding 1 μM retinoic acid and 5 μM forskolin for 5 days.

### *Cortical differentiation of human pluripotent stem cells*

In adherent conditions, hPSCs were seeded at a density of $5 \times 10^4$ cells/cm$^2$ in growth medium. At 50% confluence, the medium was gradually changed to neural basal medium (Invitrogen) containing N2 and B27 (Invitrogen). SMAD signaling inhibitors LDN193189 (Stemgent, 1 μM) and SB432542 (Tocris Biosciences, 10 μM) were added from day 1 to day 7 of neural induction. Cyclopamine (Calbiochem, 400 ng/ml) and FGF-2 (Peprotech, 10 ng/ml) were added from days 3 to 14 of differentiation. After 12–14 days, cells were mechanically passaged into poly-L-ornithine (Sigma Aldrich) and laminin (Invitrogen, 20 μg/ml) coated plates and allowed to undergo maturation for an additional 3–6 weeks. BDNF (10 ng/ml, Peprotech) was added to cultures one week after initiation of this neuronal maturation. For EB mediated neural differentiation, hPSCs were aggregated for 4 days in ultra low-attachment plates (Corning) and then seeded on Matrigel-coated plates. Cyclopamine (5 μM) and FGF-2 (10 ng/ml) were added to the cultures the following day until day 12 of neural induction. At day 14, structures with a rosette-like morphology were mechanically isolated and plated on poly-L-ornithine and laminin coated plates and allowed to undergo neuronal maturation for 4 weeks. BDNF (10 ng/ml) was added to the cultures one week after rosette isolation.

### *Gene expression analysis by RT-PCR*

Complementary DNA was synthesized from 1 μg total RNA, isolated at day 12 of neural induction and day 40 of neuronal maturation, using random primers and MultiScribe Reverse Transcriptase (Applied Biosystems) in a 20 μl reaction according to the manufacturer's recommendations. The PCR analysis was carried out with Taq DNA polymerase (New England Biolabs). Equal amounts of RNA were tested in PCR reactions under the same conditions to verify the absence of amplification of genomic DNA. The housekeeping gene glyceraldehyde-3-phosphate dehydrogenase (G3PDH) was amplified as an internal control in gene expression analysis. Primer sequences (Table 1) were obtained from the PrimerBank website (http://pga.mgh.harvard.edu/primerbank/) and synthesized by Life Technologies.

### *Immunocytochemistry*

Cultures were fixed with 4% paraformaldehyde or 3% paraformaldehyde and 2% glutaraldehyde for 10–15 min. The primary antibodies used were: mouse anti-nestin (1:50; R&D Research), rabbit anti-Pax6 (1:200; Covance), rabbit anti-BF1 (1:100, Abcam), mouse anti-Otx2 (1:50, R&D Systems), mouse anti-MAP2 (1:500, BD Biosciences), rabbit anti-glutamate (1:1500, Sigma Aldrich), rabbit anti-GABA (1:2000, Sigma Aldrich), rabbit anti VGluT1 (1:3000, Synaptic Systems), rabbit anti-TBR1 (1:1000, Millipore), rabbit anti-CUX1 (1:1000, Santa Cruz Biotechnology), rat anti-CTIP2 (1:1000, Abcam), rabbit anti-Aβ (1:500, Millipore), and rabbit anti-cleaved caspase-3 with Alexa Fluor 488 Conjugate (1:100, 1:50, Cell Signaling). For co-staining with antibodies against Aβ and glutamate or GABA, the Aβ primary antibody was conjugated to Alexa 647 dye (Invitrogen). Cultures were (with the exception of cultures stained with labeled caspase-3 and Aβ) incubated with fluorescent-labeled secondary Alexa 594-conjugated anti-rabbit and Alexa 488-conjugated anti-mouse antibodies in PBS containing 1% BSA for 1 h (1:1000, Invitrogen). Cultures were counter-stained with DAPI (Molecular Probes) and imaged using a Zeiss Axio Observer A1 inverted microscope.

### *Electrophysiology*

Whole-cell recording was made from neurons after 52 days of neuronal maturation using a patch clamp amplifier (MultiClamp 700B, Axon Instr.) under infrared differential interference contrast optics. Microelectrodes were made from borosilicate glass capillaries, with a resistance of 4–5 MW. To apply glutamate, air pulses (10 ms duration at 1 Hz) were applied by Picrospritzer III (Parker Hannifin) to a glass pipette with the tip of ~5 μm in diameter. Generally, EPSPs induced by puffed glutamate were recorded at −70 mV in current-clamp mode. For recording action potentials, cells were held at −70 mV in voltage-clamp mode. The intracellular solution for whole-cell recording of EPSPs and action potentials contained (in mM) 140 potassium gluconate, 5 KCl, 10 HEPES, 0.2 EGTA, 2 $MgCl_2$, 4 MgATP, 0.3 $Na_2GTP$ and 10 $Na_2$-phosphocreatine, pH 7.2 (adjusted with KOH).

For recording spontaneous EPSCs (sEPSCs), cells were pre-treated with the extracellular bath solution containing 50 μM picrotoxin to

**Table 1**
PCR primer sets used to validate the differential expression of the candidate genes in cortical neural progenitors and maturely differentiated cultures.

| Gene | Primer bank ID | Primer set sequenced (5′→3′) | |
|---|---|---|---|
| | | Forward | Reverse |
| PAX6 | 189083679b3 | GTAAACCGAGAGTAGCGACTCC | GCACTCCCGCTTATACTGGG |
| BF1 | 32307176b2 | GAGCGACGACGTGTTCATC | GCCGTTGTAACTCAAAGTGCTG |
| EMX1 | 28279427a1 | AAGCGCGGCTTTACCATAGAG | GGGTGAGGGTAGTTGAGCG |
| DLX2 | 4758168a3 | GCCTGAAATTCGGATAGTGAACG | AGGGGATCTCACCACTTTTCC |
| TBR1 | 22547231b1 | GCAGCAGCTACCCACATTCA | CGTGCAAGACAAGCTCGGAT |
| VGluT1 | 9945322a1 | TTTTCTGGGGCTACATTGTCAC | ACTCCGTTCTAAGGGTGGGG |
| G3PDH | 7669492a2 | TGTTGCCATCAATGACCCCTT | CTCCACGACGTACTCAGCG |

exclude an inhibitory synaptic activity and held at −70 mV in voltage-clamp mode with the intracellular solution containing (in mM) 130 $CsMeSO_4$, 7 CsCl, 10 HEPES, 1 EGTA, 4 MgATP, 0.3 $Na_2GTP$, and 10 $Na_2$-phosphocreatine, pH 7.3 (adjusted with CsOH). After recording basal sEPSC responses for 5 min, 10 μM CNQX and 100 μM D,L-APV were co-treated to test dependency of sEPSCs on AMPA- and NMDA-type of glutamate receptors. For measuring spontaneous IPSC, cells were pre-treated with the bath solution containing 10 μM CNQX and 100 μM D,L-APV and held at −70 mV with the intracellular solution containing (in mM) 137 CsCl, 10 HEPES, 1 EGTA, 4 MgATP, 0.3 $Na_2GTP$, and 10 $Na_2$-phosphocreatine, pH 7.3 (adjusted with CsOH). 50 μM picrotoxin was then treated to test a dependency of sIPSCs on GABA receptors after acquiring basal sIPSC responses for 5 min. Series resistance (15–30 MΩ) and input resistance (200 MΩ using potassium-based internal solution; 1–2 GΩ using Cs-based internal solution) were monitored throughout the whole-cell recording or compared before and after sEPSC/IPSC recordings. Off-line analysis of spontaneous EPSC and IPSC was performed by using a threshold event detection function of Clampfit software (Molecular Devices). All experiments were conducted at room temperature (22 °C–24 °C).

*Globulomer preparation*

The Aβ42 globulomer was prepared as described (Barghorn et al., 2005; Yu et al., 2009). Alkaline pretreatment of Aβ42 and preparation of low molecular weight Aβ by filtration were conducted before beginning the globulomer preparation as previously described (Yu et al., 2009). After a 18–20 h incubation, the globulomer sample was concentrated to ~500 μM via centrifugation and dialyzed into PBS before centrifuging the sample at 10,000 *g* for 10 min to remove aggregates

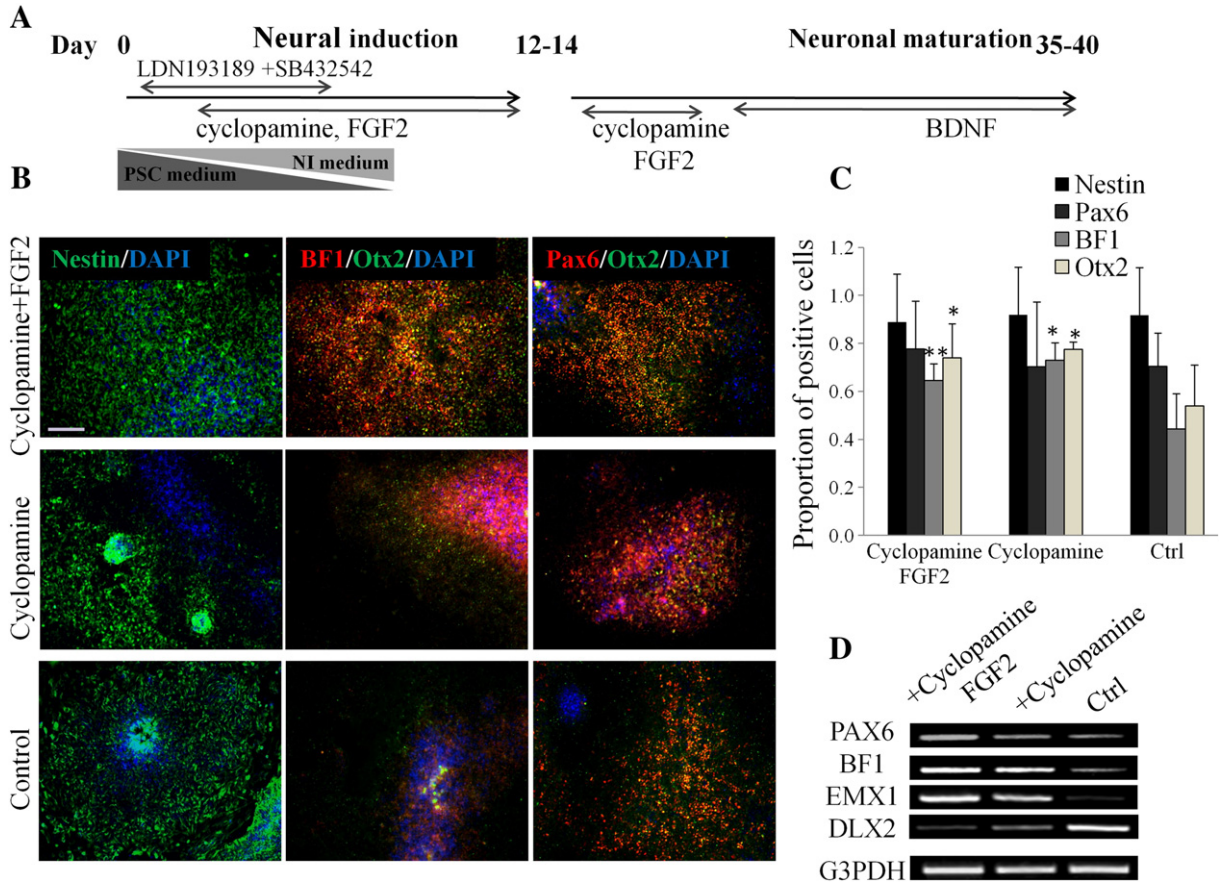


**Fig. 1.** Derivation of ventral and dorsally patterned cortical progenitors. (A) Schematic representation of the paradigm for differentiating hPSCs into cortical NPCs and glutamatergic neurons. (B) Cultures stained with antibodies against nestin, BF1, and Otx2, under conditions including the Shh signaling inhibitor cyclopamine and FGF-2, cyclopamine alone, or neither factor as indicated in the images. (C) Quantitative analysis of nestin, Pax6, BF1, and Otx2 expression in colonies differentiated in the presence or absence of cyclopamine and FGF-2 showed an increase in forebrain induction in cultures treated with cyclopamine, as indicated by BF1 expression. The differential expression of Otx2 and BF1 in cultures treated with cyclopamine, or with cyclopamine and FGF-2, was significantly different from the control conditions. The data represent an average of 368 ± 92 colonies per condition. * = $P < 0.01$, ** = $P < 0.001$. (D) Expression of BF1 and Pax6, as well as upregulation of the dorsal telencephalic marker Emx1 and downregulation of the ventral marker Dlx2, in conditions lacking endogenous Shh signaling was analyzed by RT-PCR. Scale bar: 100 μm.

in the pellet. The supernatant was saved, and the absorbance was measured at 276 nm wavelength to measure the concentration (extinction coefficient = 1390 $M^{-1}$ $cm^{-1}$).

### *Aβ42 monomer preparation*

Alkaline pretreatment of Aβ42 and preparation of LMW Aβ by filtration protocols (Teplow, 2006) were also used to prepare a monomeric solution of the peptide. This involved dissolving 1 mg of the lyophilized peptide in 2 ml of 2 mM sodium hydroxide, sonicating for 2 min, and lyophilizing. This lyophilized peptide was then dissolved in 0.166 ml hexafluoroisopropanol (HFIP) to break any existing hydrogen bonds and prevent aggregation.

### *Cell quantification*

The numbers of neurons, and globulomers associated with each neuron, were quantified manually. The numbers of cells stained with DAPI, cells positive for activated caspase-3, and the number of globulomers per field were counted automatically with ImageJ software. For cell quantifications, images of 6–12 different fields per well from three wells were acquired using a 20× objective. For neuronal cell counts, fields where MAP2 positive neurons could clearly be seen and distinguished from one other were selected without consideration of the density of neurons present in the field or neurotransmitter expression in neurons. Cell morphology and intracellular localization were carefully examined to confirm expression of marker MAP2, neurotransmitters GABA and glutamate, activated caspase-3, and transcription factors TBR1, CTIP2, and Cux1.

### *Statistics*

Differences in percentages of cells were tested by analysis of variance followed by pair-wise comparisons of group means using the Tukey–Kramer method for multiple comparisons generated by the GraphPad InStat software (GraphPad Software Inc.). Levels of significance are indicated by asterisks on the line graphs and figure legends. Differences were considered significant at $P < 0.05$. Data represent the mean values (±SD) of cell counts from triplicate samples from three independent experiments.

## Results

### *Derivation of telencephalic neural progenitor cells*

As illustrated in Fig. 1A, we first used BMP/SMAD signaling inhibitors to efficiently induce hPSC differentiation into a neural lineage (Chambers et al., 2009), and consistent with its role in development (Wilson and

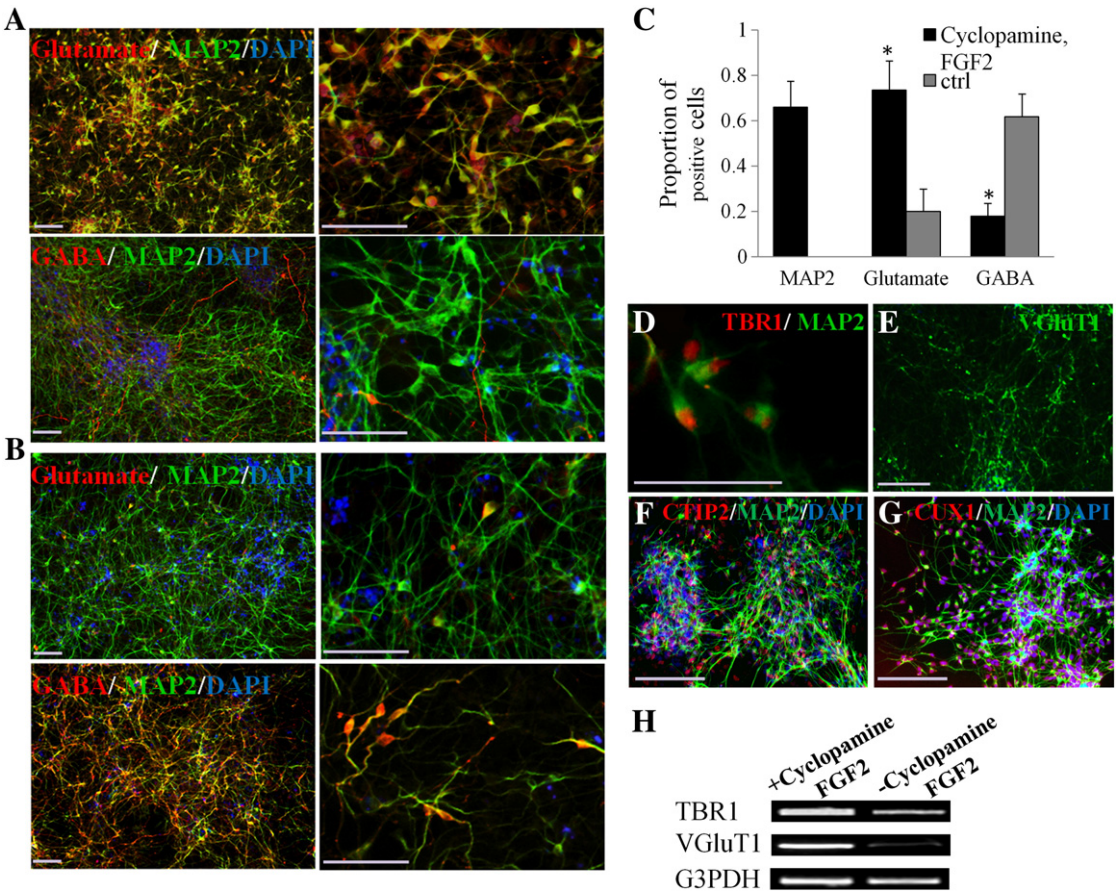


**Fig. 2.** Glutamatergic and GABAergic differentiation of hESCs. Neuronal lineage analysis of hESC-derived NPCs using antibodies against glutamate and GABA revealed that (A) dorsally regionalized neural progenitors generated by the inhibition of Shh signaling predominantly give rise to glutamatergic neurons at the expense of GABAergic specification, whereas (B) NPCs that developed in the absence of any extrinsic factors mostly adapted a ventral phenotype, giving rise to GABAergic neurons. (C) The average proportion of MAP2+ neuronal cells and the proportions of neurons expressing glutamate or GABA in each condition are presented in bar graphs with error bars indicating standard deviations. The overall difference in the number of glutamatergic and GABAergic neurons in cultures dorsally patterned in the absence of Shh signaling was statistically significant, as compared to conditions where Shh signals remained intact. The data represent an average of 203 ± 41 neurons per condition. * = $P < 0.001$. Expression of (D) the transcription factor TBR1 and (E) the vesicular glutamate transporter 1 (VGluT1) was detected in the majority of neurons differentiated from the dorsally patterned neural NPCs. (F) CTIP2 and (G) CUX1 expression confirmed the generation of neurons belonging to the deep and upper cortical layers, respectively. (H) Analysis of increased expression of TBR1 and VGluT1 in cyclopamine and FGF-2 treated neuronal cultures by RT-PCR. Scale bar: 100 μm.

Rubenstein, 2000), inhibition of the Shh signaling pathway by cyclopamine directed the resulting NPCs to a dorsal phenotype. In addition to its ventralizing effect, Shh can exert a proliferative effect on NPCs (Lai et al., 2003), and accordingly we observed a decrease in the proliferation and survival of NPCs in the presence of cyclopamine. To mitigate this loss of viability, the mitogen FGF-2, also known to exert an instructive role during telencephalic development (Ideguchi et al., 2010; Paek et al., 2009; Robel et al., 1995), was added and found to reverse the impact of cyclopamine on cell survival and proliferation (data not shown). This approach (Fig. 1A) first converted hESC cultures to a neural lineage at a high rate, as determined by nestin and Pax6 expression (Figs. 1B, C). Subsequent inhibition of Shh activity and addition of FGF-2 led to a significant increase in expression of the forebrain regionalization marker OTX2 and the telencephalic-restricted transcription factor BF1/FoxG1 (Figs. 1B, C), as compared to cultures with intact Shh signaling. To further examine the regional identity of the resulting NPCs, expression of markers associated with the ventral and dorsal forebrain was investigated. Shh signal inhibition during neural induction resulted in upregulation of the dorsal marker Emx1 and downregulation of DLX2, a marker exclusively expressed in the developing ventral telencephalon.

Subsequent neuronal lineage analysis of the dorsally patterned telencephalic NPCs revealed that approximately 74% of neurons acquired a glutamatergic phenotype, whereas GABAergic neurons comprised only 20% of the neuronal population (Figs. 2A, C). Conversely, ventral NPCs developed in the absence of cyclopamine gave rise to approximately 18% and 62% glutamatergic and GABAergic neurons, respectively (Figs. 2B, C). To further confirm the glutamatergic phenotype, we investigated the expression of the T-domain transcription factor (TBR1), which is restricted to glutamatergic neurons and excluded from GABAergic neurons in the neocortex (Hevner et al., 2001). The results illustrated clear TBR1 expression in the majority of neurons developed from dorsal NPCs (Fig. 2D). Expression of vesicular glutamate transporter 1, (VGluT1), which enables quantal release of glutamate, was also detected (Fig. 2E). In the dorsally patterned, mature cortical cultures, neurons were often positive for CUX1, a marker of cortical projection neurons in upper layers (2–4) (Fig. 2F), as well as CTIP2, a transcription factor enriched in deep layers (5–6) (Fig. 2G). The differential expression of VGluT1 and TBR1 resulting from differentiation with or without Shh inhibition was further indicated by reverse transcription polymerase chain reaction (RT-PCR) analysis (Fig. 2H).

To test the robustness of the differentiation strategy, we also implemented a protocol that involved embryoid body (EB) formation – rather than SMAD inhibition in adherent cultures – and with Shh signaling inhibition again successfully generated dorsally patterned neuronal populations expressing glutamate and VGluT1 (Figs. 3A, B). In parallel, disruption of Shh patterning activity decreased GABAergic differentiation compared to conditions where Shh signaling remained active (Figs. 3C, D). However, while the fraction of hESC-derived neurons restricted to a glutamatergic fate was comparable in the EB-based and adherent conditions, the latter culture led to a higher overall proportion of neurons within the culture. Subsequent studies were therefore conducted using neural induction by SMAD inhibition in adherent conditions.

The pioneering work by Yamanaka and colleagues (Takahashi et al., 2007) that converted somatic cells into induced pluripotent stem cells (iPSCs) has in the recent years offered the unique potential to model human diseases with patient-derived cells (Park et al., 2008). We analyzed whether the differentiation paradigm established for hESCs could extend to iPSCs. Similar to hESCs, in the presence of cyclopamine, mesenchymal stem cell (MSC) derived iPSCs (Park et al., 2008) adopted a dorsal phenotype, and glutamatergic differentiation occurred at the expense of GABAergic development (Figs. 4A–C). Additionally, TBR1 and VGluT1 expression further indicated cortical glutamatergic differentiation (Figs. 4D–F).

### *Electrophysiological assessment of cortical neurons*

To examine the functional activity of the differentiated neurons, electrophysiological recordings were performed using whole-cell patch clamping after 52 days of differentiation. Upon current injection, the dorsally patterned neurons generated from hESCs showed the

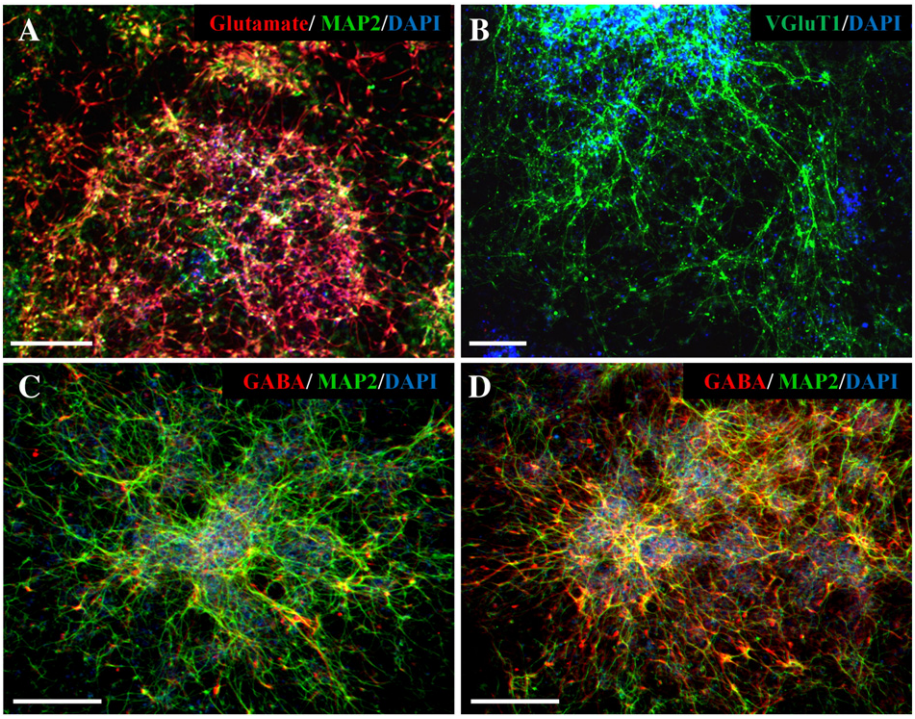


**Fig. 3.** Embryoid body (EB)-mediated neuronal differentiation. Cortical differentiation via EB-formation followed by inhibition of the ventralizing effect of Shh resulted in (A) glutamate expression in the majority of MAP2 + neurons and (B) VGluT1 expression in the majority of mature neurons after three weeks of differentiation. Blocking Shh signal transduction resulted in (C) decreased GABAergic differentiation as compared to (D) cultures where Shh signaling remained intact. Scale bar, 100 μm.

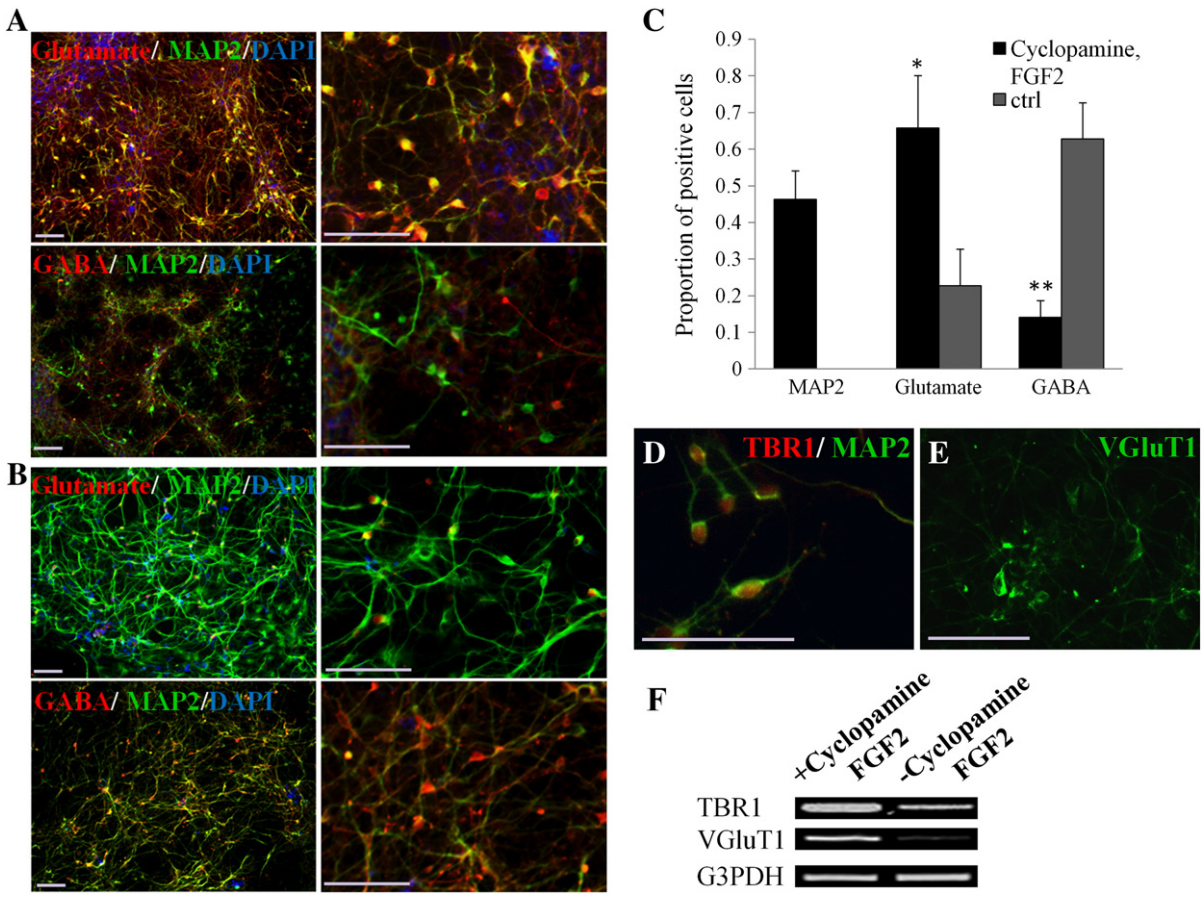


**Fig. 4.** Glutamatergic and GABAergic differentiation of human iPSCs. Glutamate and GABA immunocytochemistry in differentiated neurons generated from MSC-iPSC neural progenitors illustrated (A) an increase in the proportion of neurons expressing glutamate in the presence of cyclopamine, whereas (B) a complementary increase in GABAergic differentiation is observed when Shh signaling remained unperturbed. (C) The average proportions of MAP2 positive neuronal cells and glutamate and GABA expressing neurons generated from NPCs in the presence or absence of cyclopamine and FGF-2. The effect of cyclopamine mediated inhibition of Shh was statistically significant for glutamate and GABA expressing neurons, as compared to untreated conditions. The data represent an average of 160 ± 14 neurons per condition. * = $P < 0.001$, ** = $P < 0.0001$. (D) Expression of TBR1 and (E) VGluT1 in neurons generated from dorsal NPCs. (F) Analysis of differential expression of TBR1 and VGluT1 in the presence or absence of cyclopamine and FGF-2 by RT-PCR. Scale bar: 100 μm.

capacity to fire numerous action potentials (Fig. 5A). In addition, depolarizing voltage pulses evoked inward sodium currents, contributing to membrane excitability followed by an outward current (Fig. 5B). Moreover, the voltage-gated sodium channel blocker tetrodotoxin (TTX) blocked inward currents, providing further evidence for the presence of functional sodium channels that are responsible for action potential generation and propagation of excitatory signals by evoking release of glutamate in presynaptic glutamatergic terminals (Fig. 5B). In addition, the neurons were glutamate-responsive, as application of glutamate elicited a rapidly activating inward current (Fig. 5C). The iPSC-derived, dorsally regionalized forebrain neurons also developed into electrophysiologically mature neurons as measured by the ability to generate action potentials (Fig. 5D) and voltage-sensitive inward and outward currents (Fig. 5E). As confirmation of glutamatergic and GABAergic phenotypes, we performed whole-cell patch-clamp recording to detect spontaneous excitatory or inhibitory postsynaptic currents (sEPSCs or sIPSCs) in cortical cultures enriched in glutamatergic or GABAergic neurons in the presence of glutamate receptor antagonist and $GABA_A$ receptor antagonist, respectively. Our data clearly showed that sEPSCs in glutamatergic neurons were suppressed by co-treatment of the AMPA receptor antagonist (CNQX) and the NMDA receptor antagonist (DL-APV), confirming active glutamate-mediated synaptic transmission. Additionally, IPSCs in neuronal cultures primarily composed of the GABAergic phenotype were successfully blocked by the $GABA_A$ receptor antagonist picrotoxin verifying GABA-mediated synaptic transmission.

*Evaluation of human cortical glutamatergic neurons as a model for AD investigation*

We generated a soluble and highly stable form of Aβ oligomers termed globulomers, which are excluded from polymerization and assembly into larger fibrils (Barghorn et al., 2005). To validate the formation of globular Aβ peptide 1–42 oligomers from the non-toxic Aβ monomers, we analyzed the globulomer preparations on native polyacrylamide gel electrophoresis (PAGE) gels, which showed the intermediate oligomeric Aβ of mass 16/20 kDa and the 38/48-kDa Aβ globulomer (Fig. 6A), as previously reported (Barghorn et al., 2005). Fig. 2B illustrates the size distribution of the Aβ oligomers in a globulomer sample on a SDS-PAGE gel. Thermal denaturing of the full size Aβ globulomers subsequently resulted in SDS-PAGE bands at 16/20 kDa and 5 kDa corresponding to the pre-globulomer state and the monomeric form of Aβ, respectively (Fig. 2C).

Initially, neurons derived from adult rat hippocampal progenitors were used to determine a concentration range of this species that may be toxic, and globulomer preparations from Aβ peptide concentrations ranging from 1–5 μM were sufficient to induce cell death within 48 h (Fig. 6C).

When hESC-derived cortical cultures primarily comprised of glutamatergic neurons were treated with 2 μM globulomers, clear neuronal cell death initiated after 72 h (Fig. 6D). Analysis using caspase-3 as an apoptotic marker showed a progressive increase in glutamatergic neuron death with increasing Aβ globulomer concentration (Figs. 6E,

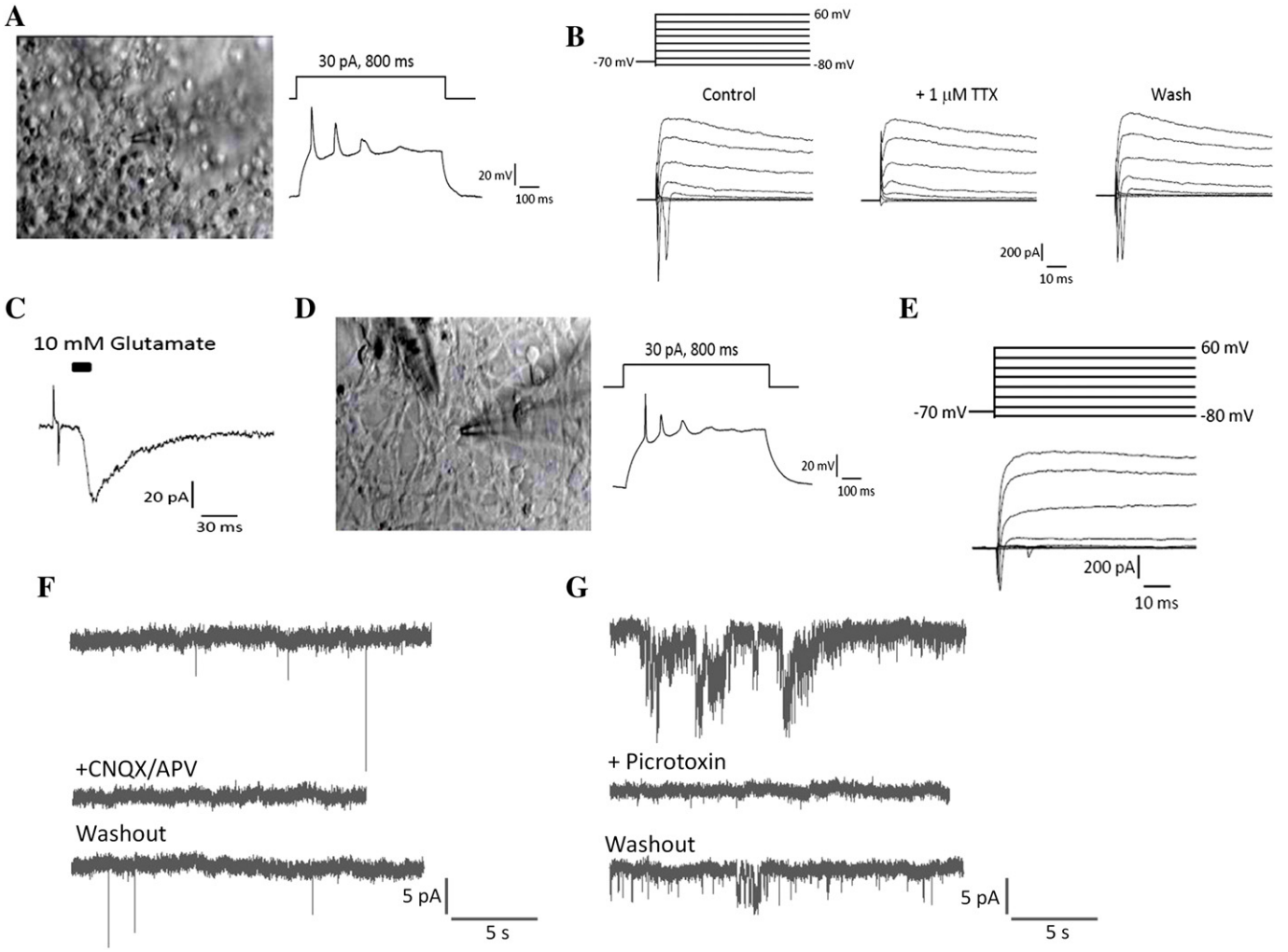


**Fig. 5.** Electrophysiological assessment of glutamatergic cultures. Electrophysiological recording from cortical neurons generated from (A–C) hESCs and (D, E) MSC-iPSCs. Phase-contrast image of (A) hESC-derived, dorsally patterned neuron during patch clamp recordings showing generation of action potentials upon 30 pA current injection after 52 days of differentiation. (B) Voltage steps (−80 mV to 60 mV) elicited inward and outward currents in neurons generated from hESCs. (B) Application of 1 μM of the sodium channel blocker tetrodotoxin completely eliminated inward currents in neurons generated from hESCs. In addition, (C) administration of 1 mM glutamate evoked inward currents at negative membrane potentials in hESC-derived neuronal populations. (D) Phase contrast image of a dorsally patterned cortical neuron generated from iPSCs firing action potentials upon 30 pA current injection after 52 days of differentiation *in vitro*. (E) In voltage-clamp mode, step depolarizing induced inward and outward currents in iPSC-derived cortical neurons. (F) Elimination of spontaneous excitatory postsynaptic currents (PSCs) in whole-cell recordings of hESC-derived cortical neurons by the AMPA receptor antagonist CNQX (10 μM) and the NMDA antagonist DL-APV (100 μM, n = 7) confirmed the glutamatergic nature of neurons generated by inhibition of Shh signaling. (G) In cultures enriched in GABAergic neurons, the $GABA_A$ receptor antagonist picrotoxin (100 μM, n = 3) successfully blocked the appearance of spontaneous inhibitory PSCs.

F), and the fraction of neurons (MAP2 +) that were glutamatergic also progressively decreased (Fig. 6G). Finally, the overall fraction of cells in the culture that were MAP2 + and glutamate + decreased in parallel, suggesting a selective neurotoxicity of Aβ globulomers against these human cortical glutamatergic neurons (Fig. 6H). By comparison, cultures treated with the same concentrations of the monomeric, non-toxic form of Aβ peptide did not show activation of caspase-3.

We also immunostained for the presence of this pre-fibrillar form of Aβ to further investigate cellular interactions, using an antibody against the Aβ fibrillar oligomeric form that also binds the soluble Aβ globulomers due to some structural similarity (Glabe, 2008). In agreement with previous studies (Barghorn et al., 2005; Verdier et al., 2004), globulomer aggregates were tightly associated with the neuronal cell membrane (Fig. 7A). Similarly, iPSC-derived neurons exhibited Aβ globulomer binding and subsequent apoptosis (data not shown). We also investigated whether neurons that had matured longer in culture may respond differentially to the Aβ globulomers, since organismal aging is the most prominent risk factor for AD, and neuronal lifetime in culture may embody some aspects of aging (Lesuisse and Martin, 2002). When hESC-derived cortical neuronal populations were matured for additional 33 days, for a total of 72 days after the initiation of differentiation, Aβ binding to the plasma membrane and the dendritic spines was significantly increased (Fig. 7B). Specifically, quantitative assessments of 100 neurons showed an increase in the average number of bound globulomer aggregates per neuron from 3 ± 1 in younger cultures to 8 ± 2 in old ($P < 0.001$), indicating that increased cell culture maturation time could offer a platform to examine how changes in neuronal membrane properties with time lead to increases in Aβ binding and pathology. Collectively, these findings illustrate that cortical neuronal cultures can be used *in vitro* to emulate and investigate AD phenotypes.

### *Examination of Aβ-induced neurotoxicity in glutamatergic and GABAergic populations*

The extent to which specific sets of neurons in the cerebral cortex are susceptible to Aβ oligomer binding and toxicity is unknown. To study neuronal phenotype sensitivities to Aβ, we exposed mature hESC-derived cultures primarily comprised of glutamatergic or GABAergic neurons to Aβ globulomer and assessed globulomer binding and neuronal

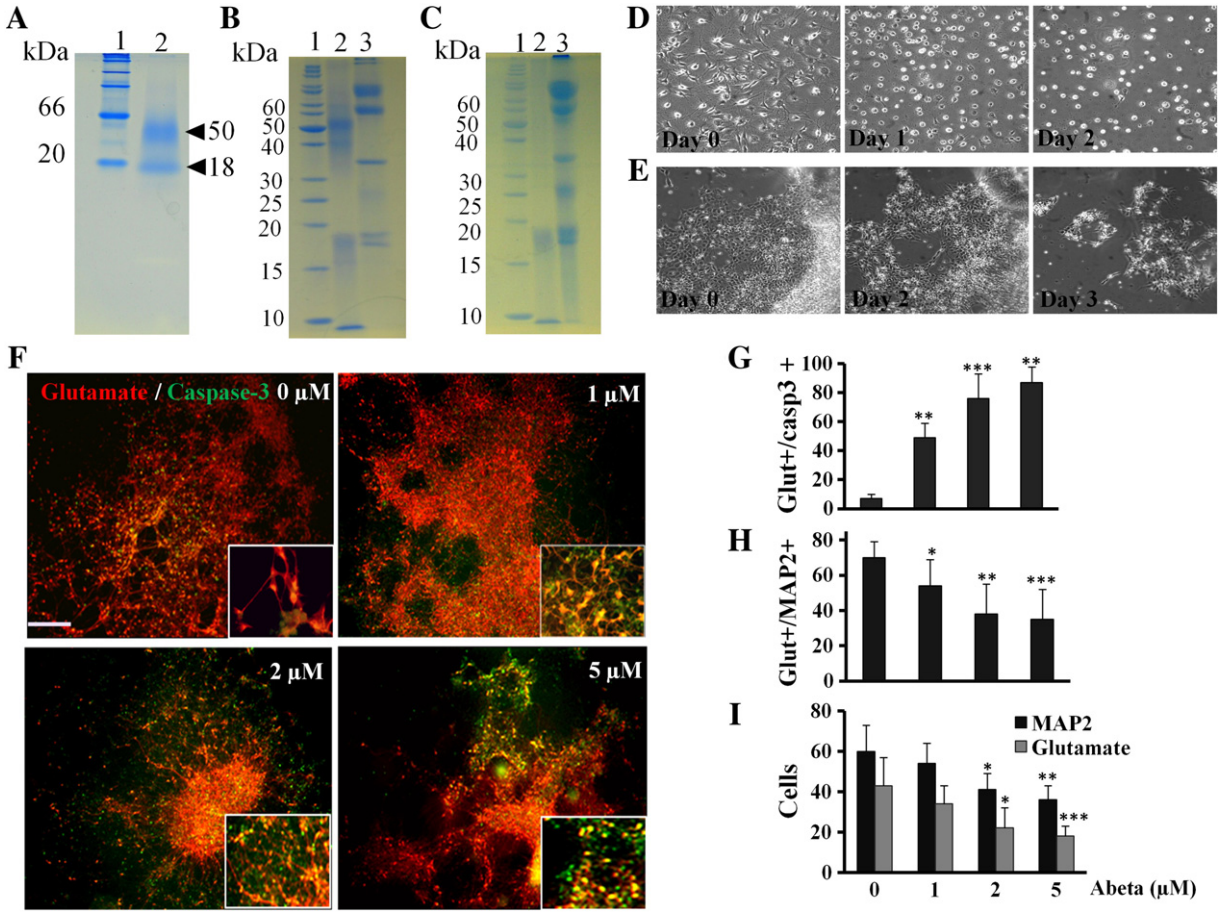


**Fig. 6.** Characterization of Aβ globulomers and characteristic response of the neuronal populations to Aβ neurotoxicity. (A) Visualization of the generated globular Aβ peptide 1–42 oligomers on Coomassie-stained, non-denaturing polyacrylamide gel electrophoresis (PAGE) gels showing the intermediate oligomeric Aβ of mass 16/20 kDa and the 38/48-kDa Aβ 1–42 globulomer. Lane 1: ladder, lane 2: Aβ globulomer sample. SDS-PAGE gel of (B) 38/48-kDa globulomer sample illustrating the size distribution of the Aβ oligomers and (C) denatured 38/48-kDa globulomer after boiling for 5 min illustrating the absence of the full size globulomer. (B,C) Bands at 16/20 kDa and 5 kDa represent the preglobulomer state and Aβ monomers, respectively. Lane 1: standard ladder, lane 2: Aβ globulomer sample, lane 3: native ladder. Representative phase contrast images of (D) adult rat hippocampal neurons and (E) hESC-derived dorsally patterned cortical neurons treated with 2 μM Aβ globulomers, exhibiting neuronal cell death after two and three days, respectively. (F) Glutamatergic neurons exhibited progressively higher cell death with increasing concentrations of the globulomeric form of Aβ, as measured by immunofluorescence staining of activated caspase-3. (G) Quantitative analysis demonstrated a concentration dependent onset of apoptosis in glutamatergic neurons treated with Aβ globulomers. The data represent an average of 152 ± 39 glutamate expressing neurons per condition. As Aβ concentrations increased, (H) the percentages of neurons with a glutamatergic fate (an average of 187 ± 33 neurons were scored per condition) and (I) the percentages of cells that were MAP2 + and glutamate expressing decreased. The increases in cell death and the decrease in the total percentages of glutamatergic neurons treated with 1, 2, and 5 μM Aβ globulomers were statistically different compared to untreated cultures. The decrease in the number of MAP2 and glutamate expressing cells was significant in conditions treated with 2, and 5 μM Aβ, as compared to culture that were not treated with Aβ. To obtain the percentages of cells expressing MAP2 +, an average of 406 ± 99 cells per condition were quantified. Percentages of cells which were glutamate expressing with a neuronal morphology were attained by quantifying an average of 390 ± 126 cells per condition.* = $P < 0.005$, ** = $P < 0.001$, *** = $P < 0.0001$. Scale bar: 100 μm.

cell death after 72 h. The levels of globulomer bound to MAP2-expressing neurons were significantly higher in glutamatergic neuronal cultures, differentiated from dorsal NPCs, than primarily GABAergic neurons, derived from ventral NPCs (Figs. 8A–B, E). Likewise, glutamatergic and GABAergic cultures exhibited substantially different levels of apoptotic cell death (Figs. 8C–E). In glutamatergic cultures exposed to Aβ, caspase-3 activation occurred in 61% of cells, compared to 33% in untreated conditions, and the fraction of overall MAP2 + neurons decreased from 56 to 31% (representing an overall 55% decrease) in response to Aβ treatment. In contrast, the GABAergic population was more resistant to Aβ, as the fraction of neurons decreased by only 17% after treatment, and neuronal caspase-3 staining was the same in treated vs. untreated cultures (Fig. 8E).

To further confirm phenotype-specific vulnerability against Aβ, we examined caspase-3 activation in glutamatergic versus GABAergic neurons in the presence or absence of 5 μM Aβ globulomers (Figs. 8F, G). Percentages of GABA and caspase-3 positive neurons were relatively unaltered after Aβ treatment in contrast to the glutamatergic neuronal populations where Aβ exposure increased the percentage of glutamate expressing neurons containing cleaved caspase-3 from 33% to 61% (Fig. 8H). In parallel, Aβ globulomers showed enhanced association with glutamatergic vs. GABAergic neurons (Figs. 8I, J). In fact, quantitative analysis of the average number of globulomers associated with individual neurons (Figs. 8K, L) suggested seven fold more Aβ binding to glutamatergic as compared to the GABAergic neuronal phenotype.

## Discussion

Numerous transgenic animal models of AD have been generated to aid in understanding mechanisms of this human disease (Gotz and Ittner, 2008), and while these models continue to provide valuable insights into disease mechanisms, non-human systems often do not fully emulate human pathophysiology as evidenced by the poor correlation between preclinical models and human clinical trials (LaFerla and Green, 2012). Analogously, overexpressing genes that influence amyloidogenesis in neurons derived from immortalized cell lines, such as the frequently used human neuroblastoma line SH-SY5Y (Belyaev et al., 2010), may not represent an accurate model to study AD as these cells are quite different from neurons that degenerate in human AD brain. Finally, tissue from AD patients is both heterogeneous and

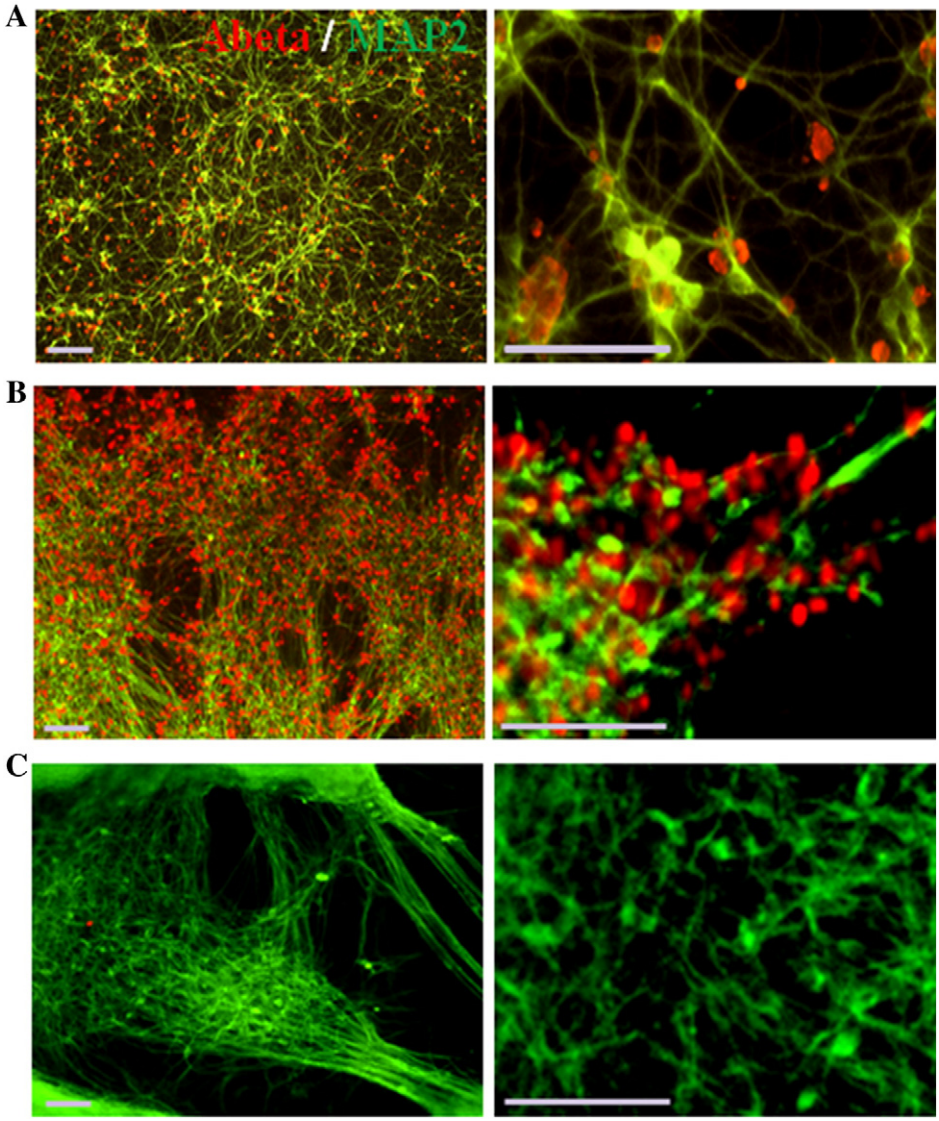


**Fig. 7.** Examination of Aβ binding affinity in aged glutamatergic neurons. Cortical neurons were treated with 5 μM Aβ globulomers for 24 h, then immunostained with an anti-Aβ antibody. Binding of Aβ globulomers on the surface of MAP2 + neurons at (A) day 25, as compared to (B) day 58 of neuronal maturation illustrates enhanced interaction and binding of Aβ to aged neurons in culture. (C) The untreated control without Aβ showed no signal. Scale bar, 100 μm.

limited. Such challenges can potentially be addressed by using models of hPSC-derived neuronal phenotypes that undergo degeneration in AD for basic investigation or therapeutic development. In this study, we established an efficient differentiation paradigm to generate human glutamatergic neurons and begun to evaluate their potential as an AD model.

Recent studies (Israel et al., 2012; Qiang et al., 2011; Yagi et al., 2012) have successfully generated neurons from fibroblasts of familial and sporadic AD patients by cellular reprogramming. That said, neuronal models based on iPSCs or direct reprogramming of cells from AD patients likely preclude the possibility of introducing a pathological AD environment to already mature and healthy neuronal populations, and thereby complicate efforts to develop preventive measures at early stages of the disease. The cholinergic system is also affected by AD (Francis et al., 1999), and a model of cholinergic neurons derived from hESCs has recently been established (Bissonnette et al., 2011). However, human cortical glutamatergic neurons, which are strongly involved in the neuropathology of AD (Francis et al., 1993; Greenamyre et al., 1988), have remained largely unexplored in biomedical investigations of this disease.

During forebrain development, Shh signaling contributes to the establishment of dorsal and ventral cortical regions, leading to the generation of glutamatergic and GABAergic neurons, respectively (Ericson et al., 1995; Wilson and Rubenstein, 2000). Based on these findings, differentiation protocols of ESCs have used Shh pathway inhibition to obtain NPCs with distinct telencephalic regional identities (Gaspard et al., 2008; Shi et al., 2012). However, a recent contrasting study indicated that human ESCs undergo a self-organized formation of dorsal telencephalic neural progenitors without extrinsic inhibition of the Shh pathway (Li et al., 2009).

In this study, we show that active manipulation with a Shh antagonist can lead to a more efficient specialization of dorsal telencephalic NPCs, and in turn efficiently yield glutamate expressing neurons. Conversely, in the absence of Shh inhibition, the resulting NPCs adapted a ventral phenotype and primarily gave rise to GABAergic neurons. In addition, FGF-2 exerts a wide range of activities during early brain development, including stimulation of neural precursor proliferation, neuronal differentiation, neurite outgrowth of hippocampal and cortical neurons, and enhancement of neuronal survival (Gremo and Presta, 2000). FGF-2 may also play a role in forebrain patterning, as it has been suggested to regulate Otx2 expression in the developing telencephalon (Robel et al., 1995). In contrast to the previous studies of ESC cortical differentiation (Gaspard et al., 2008; Shi et al., 2012),

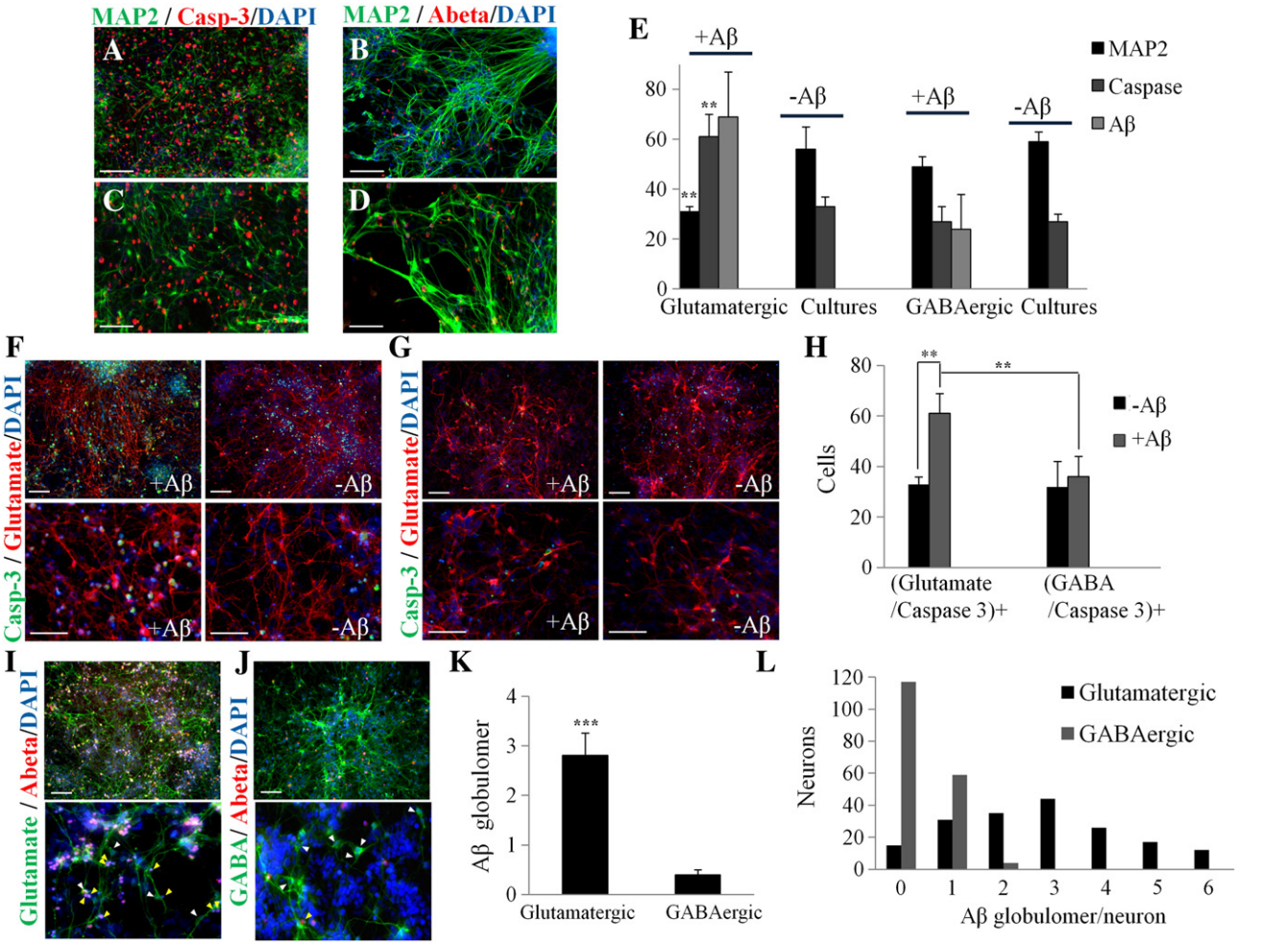


**Fig. 8.** Neuronal phenotype-specific Aβ binding and neurotoxicity. Following exposure to globulomers, Aβ and MAP2 staining of cultures derived from dorsal and ventral NPCs – which mainly gave rise to glutamatergic and GABAergic populations, respectively – illustrated enhanced binding of Aβ to the (A) glutamatergic populations as compared to (B) GABAergic cultures. The levels of caspase-3 activation were elevated in (C) glutamatergic versus (D) GABAergic cultures. (E) Quantitative analysis of the percentages of MAP2 expressing neurons, number of globulomer aggregates divided by number of cells stained with DAPI, and percentage of cells containing activated caspase-3 in glutamatergic and GABAergic neuronal populations in the presence or absence of Aβ globulomers (5 μM) for 72 h. (E) In conditions treated with 5 μM Aβ, the overall changes in percentages of MAP2 + and activated caspase-3 + neurons in glutamatergic cultures were significantly different from GABAergic cultures. The data represent an average of 1201 ± 413 cells per condition. ** = $P < 0.001$. Analysis of activated caspase-3 in (F) glutamatergic and (G) GABAergic neurons in the presence or absence of Aβ globulomers as indicated in images. (H) Quantification of the percentages of glutamatergic and GABAergic neurons positive for activated caspase-3, confirming a statistically significant increase in Aβ-induced toxicity in glutamate expressing neurons as compared to the GABAergic neuronal populations. ** = $P < 0.001$. Illustration of Aβ binding to (I) glutamatergic and (J) GABAergic neurons. Scale bar: 100 μm. White and yellow arrowheads in the lower panels show cell bodies and globulomers associated with neurons, respectively. Bar graphs presenting (K) the average number of globulomers per glutamatergic of GABAergic neuron (499 ± 95 neurons per condition were analyzed) and (L) the distribution of individual glutamatergic and GABAergic neurons with various numbers of associated globulomers (180 neurons were analyzed per condition). The average number of globulomers/neuron associated with glutamatergic neurons versus GABAergic neurons was significantly different, *** = $P < 0.0001$.

we found that FGF-2 could be used to greatly enhance forebrain NPC survival and proliferation, as well as promote a downstream increase in the number of human cortical neurons.

We used the resulting cortical glutamatergic neurons, derived from the H1 hESC line as well as a MSC-iPSC line, to study AD pathology *in vitro* by showing severe toxicity for a pre-fibrillar form of Aβ that may be present in patients suffering from AD (Kuo et al., 1996). Interestingly, the glutamatergic model illustrated enhanced binding of Aβ globulomers to individual neurons with increased time in culture, which may offer some parallels with neuronal aging *in vivo* (Lesuisse and Martin, 2002). The mechanisms and binding partners involved in the association of Aβ oligomers with cortical neurons have not been identified, though a number of membrane associated proteins – including NMDA receptors, integrins, and proteoglycans – have been identified as potential binding proteins in various types of neurons (Verdier et al., 2004). An alternative hypothesis for Aβ-induced cytotoxicity involves age-related disruption of the cell surface membrane through alterations of the membrane lipid layer fluidity that eventually lead to apoptotic or necrotic cell death (Igbavboa et al., 1996; Kremer et al., 2000). In either case, the model presented in this study may offer a platform for advancing our understanding of age-related association and binding of Aβ to the plasma membranes as a potential point of intervention.

Our Aβ neurotoxicity analysis indicated a selective pathology against glutamatergic neurons, as the fraction of neurons of this phenotype decreased with increasing Aβ concentrations. This effect may be related to their capacity to bind the globulomers (Fig. 8E). In fact, it has been suggested by studies performed in neuronal cell lines and rat primary hippocampal and cortical cultures that differential sensitivity to Aβ is associated with cell membrane Aβ binding (Simakova and Arispe, 2007). However, the binding affinity and selective sensitivity of different types of neurons to neurotoxic effects of Aβ remain a matter of debate and must be studied in greater detail.

There are differing reports on the susceptibility of GABAergic neurons to AD pathology. For example, hippocampal GABAergic neurons are susceptible to Aβ toxicity *in vitro* and decrease in number in the AD TgCRND8 mouse (Krantic et al., 2012; Pike and Cotman, 1993), and small GABAergic neurons were vulnerable to Aβ pentapeptide in

primary rat basal forebrain cultures (Pakaski et al., 1998). Other studies in mice overexpressing apolipoprotein E4, a major genetic risk factor for AD, have shown a tauopathy mediated impairment of hippocampal GABAergic interneurons (Andrews-Zwilling et al., 2010), which may be Aβ-independent (Huang, 2010). By contrast, cortical GABAergic neurons were relatively spared in a study of postmortem tissue from AD patients (Rossor et al., 1982). A recent study suggested that aberrant network activity in human APP transgenic mice may arise from decreased expression of a voltage-gated sodium channel subunit in cortical parvalbumin subtype GABAergic interneurons (Verret et al., 2012), though GABAergic neurodegeneration was not specifically examined in this study. Given stark differences in the sensitivity of human and mouse brain to pathological alleles from familial forms of AD, it is important to examine Aβ biology and pathology in the types of human neurons directly impacted by AD. To our knowledge, however, the cell-type specific behavior of human cortical neurons has not been explored in an AD neurotoxic environment.

To shed some light on neuronal phenotype-specific vulnerability in AD, we present a human cell model of glutamatergic and GABAergic neuronal cultures and illustrate that the glutamatergic neurons are comparatively more susceptible to Aβ toxicity. These results with human cells agree more closely with the cerebral cortex of postmortem human AD patients (Rossor et al., 1982) than with animal studies conducted to date.

The cortical culture systems presented in this study provide an opportunity to study the underlying mechanisms of the differential response of human neuronal phenotypes to the most neurotoxic agent in AD. Future advances in the generation and assessment of neurons representative of the distinct layers of the cortex may further aid studies of neuronal vulnerability to AD pathology, and in general hPSC-derived cortical neuronal cultures may lay the groundwork for more effective discovery of AD diagnostics or pharmacological intervention.

## Conclusions

We have examined the effects of a pre-fibrillar form of Aβ on human pluripotent stem cell derived glutamatergic neurons, which comprise a large fraction of the human cortical regions that undergo severe degeneration in AD. Our study clearly shows a human cortical neuronal phenotype-dependent binding of and susceptibility to Aβ globulomers. The ability to reproducibly generate large quantities of different human neuronal subtypes will help investigations of cellular and biochemical dynamics during early to late stages of AD-induced neurodegeneration, which may aid in the identification of new diagnostic markers and ultimately new preventive treatments.

## Acknowledgments

This work was supported by CIRM Award TG2-01164 and CIRM grant RT2-02022. We thank Dr. Sudhir Sharma and Ms Aradhana Verma for providing technical assistance with this work and Ms Analisa Nazari for neuronal cell quantification.

## References

Andrews-Zwilling, Y., et al., 2010. Apolipoprotein E4 causes age- and Tau-dependent impairment of GABAergic interneurons, leading to learning and memory deficits in mice. J. Neurosci. 30, 13707–13717.
Barghorn, S., et al., 2005. Globular amyloid beta-peptide oligomer — a homogenous and stable neuropathological protein in Alzheimer's disease. J. Neurochem. 95, 834–847.
Belyaev, N.D., et al., 2010. The transcriptionally active amyloid precursor protein (APP) intracellular domain is preferentially produced from the 695 isoform of APP in a beta-secretase-dependent pathway. J. Biol. Chem. 285, 41443–41454.
Bissonnette, C.J., et al., 2011. The controlled generation of functional basal forebrain cholinergic neurons from human embryonic stem cells. Stem Cells 29, 802–811.
Chambers, S.M., et al., 2009. Highly efficient neural conversion of human ES and iPS cells by dual inhibition of SMAD signaling. Nat. Biotechnol. 27, 275–280.
Ericson, J., et al., 1995. Sonic hedgehog induces the differentiation of ventral forebrain neurons: a common signal for ventral patterning within the neural tube. Cell 81, 747–756.
Francis, P.T., et al., 1999. The cholinergic hypothesis of Alzheimer's disease: a review of progress. J. Neurol. Neurosurg. Psychiatry 66, 137–147.
Francis, P.T., et al., 1993. Cortical pyramidal neurone loss may cause glutamatergic hypoactivity and cognitive impairment in Alzheimer's disease: investigative and therapeutic perspectives. J. Neurochem. 60, 1589–1604.
Gaspard, N., et al., 2008. An intrinsic mechanism of corticogenesis from embryonic stem cells. Nature 455, 351–357.
Glabe, C.G., 2008. Structural classification of toxic amyloid oligomers. J. Biol. Chem. 283, 29639–29643.
Gotz, J., Ittner, L.M., 2008. Animal models of Alzheimer's disease and frontotemporal dementia. Nat. Rev. Neurosci. 9, 532–544.
Greenamyre, J.T., et al., 1988. Glutamate transmission and toxicity in Alzheimer's disease. Prog. Neuropsychopharmacol. Biol. Psychiatry 12, 421–430.
Gremo, F., Presta, M., 2000. Role of fibroblast growth factor-2 in human brain: a focus on development. Int. J. Dev. Neurosci. 18, 271–279.
Hevner, R.F., et al., 2001. Tbr1 regulates differentiation of the preplate and layer 6. Neuron 29, 353–366.
Huang, Y., 2010. Abeta-independent roles of apolipoprotein E4 in the pathogenesis of Alzheimer's disease. Trends Mol. Med. 16, 287–294.
Ideguchi, M., et al., 2010. Murine embryonic stem cell-derived pyramidal neurons integrate into the cerebral cortex and appropriately project axons to subcortical targets. J. Neurosci. 30, 894–904.
Igbavboa, U., et al., 1996. Increasing age alters transbilayer fluidity and cholesterol asymmetry in synaptic plasma membranes of mice. J. Neurochem. 66, 1717–1725.
Israel, M.A., et al., 2012. Probing sporadic and familial Alzheimer's disease using induced pluripotent stem cells. Nature 482, 216–220.
Krantic, S., et al., 2012. Hippocampal GABAergic neurons are susceptible to amyloid-beta toxicity in vitro and are decreased in number in the Alzheimer's disease TgCRND8 mouse model. J. Alzheimers Dis. 29, 293–308.
Kremer, J.J., et al., 2000. Correlation of beta-amyloid aggregate size and hydrophobicity with decreased bilayer fluidity of model membranes. Biochemistry 39, 10309–10318.
Kuo, Y.M., et al., 1996. Water-soluble Abeta (N-40, N-42) oligomers in normal and Alzheimer disease brains. J. Biol. Chem. 271, 4077–4081.
LaFerla, F.M., Green, K.N., 2012. Animal models of Alzheimer disease. Cold Spring Harb. Perspect. Med. 2.
Lai, K., et al., 2003. Sonic hedgehog regulates adult neural progenitor proliferation in vitro and in vivo. Nat. Neurosci. 6, 21–27.
Lazarczyk, M.J., et al., 2012. Preclinical Alzheimer disease: identification of cases at risk among cognitively intact older individuals. BMC Med. 10, 127.
Lesuisse, C., Martin, L.J., 2002. Long-term culture of mouse cortical neurons as a model for neuronal development, aging, and death. J. Neurobiol. 51, 9–23.
Li, X.J., et al., 2009. Coordination of sonic hedgehog and Wnt signaling determines ventral and dorsal telencephalic neuron types from human embryonic stem cells. Development 136, 4055–4063.
Naslund, J., et al., 2000. Correlation between elevated levels of amyloid beta-peptide in the brain and cognitive decline. JAMA 283, 1571–1577.
Paek, H., et al., 2009. FGF signaling is strictly required to maintain early telencephalic precursor cell survival. Development 136, 2457–2465.
Pakaski, M., et al., 1998. Vulnerability of small GABAergic neurons to human beta-amyloid pentapeptide. Brain Res. 796, 239–246.
Palmer, T.D., et al., 1999. Fibroblast growth factor-2 activates a latent neurogenic program in neural stem cells from diverse regions of the adult CNS. J. Neurosci. 19, 8487–8497.
Park, I.H., et al., 2008. Disease-specific induced pluripotent stem cells. Cell 134, 877–886.
Pike, C.J., Cotman, C.W., 1993. Cultured GABA-immunoreactive neurons are resistant to toxicity induced by beta-amyloid. Neuroscience 56, 269–274.
Qiang, L., et al., 2011. Directed conversion of Alzheimer's disease patient skin fibroblasts into functional neurons. Cell 146, 359–371.
Robel, L., et al., 1995. Fibroblast growth factor 2 increases Otx2 expression in precursor cells from mammalian telencephalon. J. Neurosci. 15, 7879–7891.
Rossor, M.N., et al., 1982. A post-mortem study of the cholinergic and GABA systems in senile dementia. Brain 105, 313–330.
Shi, Y., et al., 2012. Human cerebral cortex development from pluripotent stem cells to functional excitatory synapses. Nat. Neurosci. 15 (477–86), S1.
Simakova, O., Arispe, N.J., 2007. The cell-selective neurotoxicity of the Alzheimer's Abeta peptide is determined by surface phosphatidylserine and cytosolic ATP levels. Membrane binding is required for Abeta toxicity. J. Neurosci. 27, 13719–13729.
Takahashi, K., et al., 2007. Induction of pluripotent stem cells from adult human fibroblasts by defined factors. Cell 131, 861–872.
Teplow, D.B., 2006. Preparation of amyloid beta-protein for structural and functional studies. Methods Enzymol. 413, 20–33.
Verdier, Y., et al., 2004. Amyloid beta-peptide interactions with neuronal and glial cell plasma membrane: binding sites and implications for Alzheimer's disease. J. Pept. Sci. 10, 229–248.
Verret, L., et al., 2012. Inhibitory interneuron deficit links altered network activity and cognitive dysfunction in Alzheimer model. Cell 149, 708–721.
Viola, K.L., et al., 2008. Why Alzheimer's is a disease of memory: the attack on synapses by A beta oligomers (ADDLs). J. Nutr. Health Aging 12, 51s–57s.
Wilson, S.W., Rubenstein, J.L., 2000. Induction and dorsoventral patterning of the telencephalon. Neuron 28, 641–651.
Yagi, T., et al., 2012. Modeling familial Alzheimer's disease with induced pluripotent stem cells. Rinsho Shinkeigaku 52, 1134–1136.
Yu, L., et al., 2009. Structural characterization of a soluble amyloid beta-peptide oligomer. Biochemistry 48, 1870–1877.